J. Opt. A: Pure Appl. Opt. **7** (2005) S38–S43 doi:10.1088/1464-4258/7/2/005

Ab initio analysis of frequency selective surfaces based on conventional and complementary split ring resonators

R Marqués[1], J D Baena[1], M Beruete[2], F Falcone[2], T Lopetegi[2], M Sorolla[2], F Martín[3] and J Garcia[3]

[1] Departamento de Electrónica y Electromagnetismo, Universidad de Sevilla, 41012-Sevilla, Spain
[2] Departamento de Ingeniería Eléctrica y Electrónica, Universidad Pública de Navarra, 31006-Pamplona, Spain
[3] Departamento d'Enginyeria Electrónica, Universitat Autónoma de Barcelona, 08193-Barcelona, Spain

E-mail: marques@us.es

Received 21 May 2004, accepted for publication 30 November 2004
Published 20 January 2005
Online at stacks.iop.org/JOptA/7/S38

Abstract
Frequency selective surfaces (FSSs) made up of periodic arrays of split ring resonators (SRRs) are analysed. This analysis includes complementary screens, or complementary SRR-FSSs (CSRR-FSSs). It is shown that these FSSs show a dual behaviour, with a stop/pass band behaviour at the frequency of resonance of the SRRs/CSRRs. Cross-polarization effects in the SRR and the CSRR are considered, and it is shown that they permit resonance to occur for normally incident plane wave excitation. This latter property of SRRs and CSRRs also implies that the FSSs considered may act as polarizers and polarization converters as well. An analytical theory, valid for perfectly conducting and infinitely thin screens, is proposed for the SRR-FSSs and CSRR-FSSs. These approximations are valid in the microwave and millimetre-wave range, and up to the terahertz range.

Keywords: frequency selective surfaces, split ring resonators, Babinet principle

1. Introduction

Frequency selective surfaces (FSSs) are well known devices for use at microwave frequencies [1, 2]. Usually they consist of a periodic array of resonant metallic elements or apertures on a metallic screen. According to diffraction theory, for secondary-grating lobe suppression the size and periodicity of the resonant elements should be smaller than the wavelength of the incident radiation. Otherwise, the resonant optical properties of the FSS may be related to the coupling between adjacent elements, thus depending on the angle of incidence of the incoming radiation. Recently, a novel resonant structure, the so-called split ring resonator (SRR) [3], has been proposed for the design of artificial magnetic media with unusual electromagnetic properties. The main characteristics of this new *particle* are the small electrical size at resonance, and a strong magnetic moment near this resonance. These properties have been successfully applied to the design of artificial negative magnetic permeability media [3] and left-handed metamaterials [4]. It has also been reported that SRRs show cross-polarization effects [5]. Thus, a strong electric dipole always appears at resonance, together with the aforementioned magnetic moment. This electric dipole lies in the plane of the SRR, and is directed along the y-axis of the particle (see figure 1). Therefore this effect allows SRR resonance excitation by a normally incident plane wave of the appropriate polarization [6]. As will be shown in the following, these properties make the SRRs very well suited for FSS design.

As was already mentioned, most of present applications of SRRs are in the design of bulk artificial magnetic media by means of three-dimensional arrays of these elements. However, SRR applications are not necessarily restricted

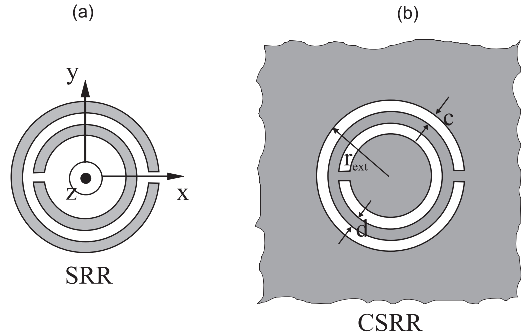

Figure 1. Geometries of the SRR (a) and the CSRR (b).

to this. In fact, the properties and applications of planar metasurfaces made by arraying these particles in two dimensions have been recently explored [7, 8]. In particular, the usefulness of these arrays as FSSs has been recently demonstrated [8]. As is usual in non-connected FSSs [2], SRR-FSSs show a stop band behaviour near the frequency of resonance of the constitutive elements. However, for many applications, just the dual behaviour, i.e. a pass band characteristic, is desired. FSSs with this behaviour can be easily designed by using the Babinet principle [8]. This implies the use of the *particle complementary* to the SRR, that is, the CSRR shown in figure 1. In fact, the two FSSs can be analysed by the same procedure if infinitely thin perfectly conducting screens are considered. This approximation is usually assumed at microwave frequencies, where metals behave as almost perfect conductors. It usually holds until the terahertz range is reached [7]. As is well known, such an approximation is not justified at optical frequencies. Nevertheless, even at these frequencies, an analytical theory of SRR-FSSs and CSRR-FSSs based on the aforementioned approximation can be useful as a starting point for the analysis, or to check the validity of the usual hypothesis on the SRR behaviour at these frequencies. As was already mentioned, in order to avoid higher order grating lobes, FSSs should be designed with element sizes and spacing smaller than a half of the free space wavelength at the frequency of operation. The SRRs and CSRRs are actually sub-wavelength resonators; therefore they can easily fulfil this requirement.

This paper presents an *ab initio* analytical theory for the design of SRR-made and CSRR-made FSSs. The validity of this analysis is restricted to infinitely thin metallic perfectly conducting screens in free space, and to SRR/CSRR sizes much smaller than the free space wavelength. As will be shown, under these assumptions the analysis can be simplified by using the surface admittance concept and the Babinet principle. The first restriction implies that the usual FSSs made by photo-etching a metallic pattern on a low loss dielectric board can only be approximately analysed by using the proposed approach (the lower the dielectric constant and the thinner the board, the better the approximation). Additional theoretical efforts will be needed in order to formulate a complete theory valid for such *practical* FSSs. However, it can be reasonably expected that most of the qualitative results from the proposed theory will still be valid for them. The second restriction is not a practical one since, as was already mentioned, it is a usual requirement in FSS design.

The results of the proposed theory have been quantitatively tested by means of some preliminary simulations in a commercial electromagnetic solver. The results of this comparison are stimulating, showing a reasonable qualitative and quantitative agreement. It is worth mentioning that, although the transmission and reflection characteristics of the structures analysed could be computed by using available commercial software, this mere brute force approach will not provide any insight into the physics of the devices studied, nor any guide for the design. In contrast, the present theory provides, with *zero computer time*, an accurate picture of the main qualitative effects (resonances, polarization of the transmitted and reflected waves, ...), as well as an accurate approximation to the quantitative behaviour of the structures analysed. Thus, it provides a good guide for the design; commercial software is still useful, within this strategy, as a fine tuning tool.

2. Analysis

In the following we will consider the behaviour of a FSS made up of a regular array of SRRs in the long wavelength limit, i.e. when the FSS peridiocity can be considered small in comparison with the operating wavelength. As was pointed out in the introduction, this condition can be easily fulfilled owing to the small electrical size of the SRRs. Next, the behaviour of the complementary screen, i.e. a FSS made up of a regular array of CSRRs etched on a thin metallic plate, will be analysed on the basis of the well known Babinet principle.

2.1. SRR polarizabilities

The behaviour of a SRR (see figure 1(a)) near its first resonance is well known. It mainly behaves as an LC resonator driven by an external magnetic and/or electric field of the appropriate polarization [5, 10]. Cross-polarization effects are present in such a particle [5, 6, 9], so a magnetic and an electric dipole arise simultaneously as a consequence of the particle excitation. This behaviour is summarized in terms of the four particle polarizabilities α_{xx}^{ee}, α_{yy}^{ee}, α_{yz}^{em}, and α_{zz}^{mm} [10]:

$$m_z = \alpha_{zz}^{mm} B_z^{\mathrm{ext}} - \alpha_{yz}^{em} E_y^{\mathrm{ext}} \tag{1}$$

$$p_y = \alpha_{yy}^{ee} E_y^{\mathrm{ext}} + \alpha_{yz}^{em} B_z^{\mathrm{ext}} \tag{2}$$

$$p_x = \alpha_{xx}^{ee} E_x^{\mathrm{ext}}, \tag{3}$$

where the axis orientation can be seen in figure 1, and the symmetries imposed by the Onsager principle on the generalized susceptances [11] have been explicitly taken into account. In (1)–(3) $\mathbf{E}^{\mathrm{ext}}$ and $\mathbf{B}^{\mathrm{ext}}$ are the externally applied fields. The theory leading to the aforementioned polarizabilities is developed in [10]. Three of the four polarizabilities—α_{yy}^{ee}, α_{yz}^{em}, and α_{zz}^{mm}—have a resonant behaviour with a strong peak at the frequency of resonance, ω_0, of the SRR. The remaining polarizability, α_{xx}^{ee}, is approximated as that of a metal disk of external radius equal to those of the SRRs [12]. Following the theory reported in [5] and [10], suitable expressions for lossless SRR polarizabilities in free space are

$$\alpha_{zz}^{mm} = \frac{\pi^2 r_0^4}{L} \left(\frac{\omega_0^2}{\omega^2} - 1 \right)^{-1} \tag{4}$$

$$\alpha_{xx}^{ee} = \varepsilon_0 \tfrac{16}{3} r_{\rm ext}^3 \tag{5}$$

$$\alpha_{yz}^{em} = -2{\rm i}\omega_0 \pi r_0^3 d_{\rm eff} C_{\rm pul} \frac{\omega_0}{\omega}\left(\frac{\omega_0^2}{\omega^2} - 1\right)^{-1} \tag{6}$$

$$\alpha_{yy}^{ee} = \varepsilon_0 \frac{16}{3} r_{\rm ext}^3 + 4\omega_0^2 r_0^2 d_{\rm eff}^2 C_{\rm pul}^2 L \left(\frac{\omega_0^2}{\omega^2} - 1\right)^{-1}, \tag{7}$$

where $r_{\rm ext}$ is the external radius of the SRR; L is the inductance of an *average* ring of mean radius $r_0 = r_{\rm ext} - c - d/2$ and width c; and $C_{\rm pul}$ is the capacitance per unit length between the rings. The frequency of resonance ω_0 is given by [5]

$$\omega_0 = \sqrt{\frac{2}{\pi r_0 L C_{\rm pul}}}. \tag{8}$$

It is easily realized that this frequency corresponds to the LC resonator formed by the SRR inductance L, and the overall capacitance of the upper and lower SRR halves connected in series: $C = \pi r_0 C_{\rm pul}/2$. The effective distance $d_{\rm eff}$ in (6) and (7) is defined as follows: this effective distance multiplied by the unit length charge on each ring should give the linear density of electric polarization along both rings [5]. Methods for the effective computation of L and $C_{\rm pul}$ are reported in [10]. The effective distance $d_{\rm eff}$ can be evaluated from the charge distribution of two parallel metallic strips of width c, separated by a distance d. However, a first-order approximation for this quantity is simply the distance between the centres of the two strips: $d_{\rm eff} \simeq c + d$. Ohmic losses can be introduced in (4)–(8) by introducing a complex inductance $\hat{L} = L + {\rm i}R/\omega$ which incorporates the ohmic resistance along the rings. Approximate expressions for R are provided in [10].

2.2. The surface admittance approach for the FSS

Let us now consider a surface made up of a square array of equally oriented SRRs (see figure 2). From the aforementioned qualitative considerations, it can be expected that this FSS will provide a strong reflectivity near the SRR resonances (for the appropriate polarization of the incident field), being otherwise almost transparent. If the first resonance, ω_0, is considered, the appropriate polarizations include non-vanishing B_z and/or E_y incident fields. Let the lattice constant be $a \ll \lambda$, where λ is the wavelength of the incident radiation. Then we are in the realm of the long wavelength limit, and the FSS can be approximated by a surface density of magnetic polarization $\mathbf{M}_{\rm s} = m_z a^{-2}\hat{\mathbf{z}}$ superimposed on a surface density of electric polarization $\mathbf{P}_{\rm s} = p_x a^{-2}\hat{\mathbf{x}} + p_y a^{-2}\hat{\mathbf{y}}$. This last polarization sheet is, in fact, equivalent to a surface density of electric current $\mathbf{J}_{\rm s,p} = -{\rm i}\omega\mathbf{P}$. In addition, from the well known equivalence principle, the aforementioned surface density of magnetization, $\mathbf{M}$, is equivalent to a surface density of electric current $\mathbf{J}_{\rm s,m} = \nabla \times \mathbf{M}_{\rm s} = -\hat{z} \times \nabla M_{{\rm s},z}$ [12]. Thus, the whole FSS is equivalent to a sheet of current with surface density $\mathbf{J}_{\rm s} = \mathbf{J}_{\rm s,p} + \mathbf{J}_{\rm s,m}$.

This surface current density can be obtained from the SRR polarizabilities (1)–(3), provided that the external fields acting on the SRRs are known. The external fields on each SRR come from the incident radiation, as well as from the surrounding SRRs. Thus they can be deduced from the mean fields at the current sheet by the appropriate homogenization procedure. The first approximation is to simply take these external fields equal to the mean fields at the FSS. Since we are mainly interested in a first-order theory this approximation, strictly valid only for sparse distributions of SRRs, will be assumed throughout this work. More accurate approximations will be the subject of subsequent works. Using the above approach, from (1)–(3) and taking into account the Faraday's law $\nabla \times \mathbf{E} = {\rm i}\omega\mathbf{B}$, it is deduced that

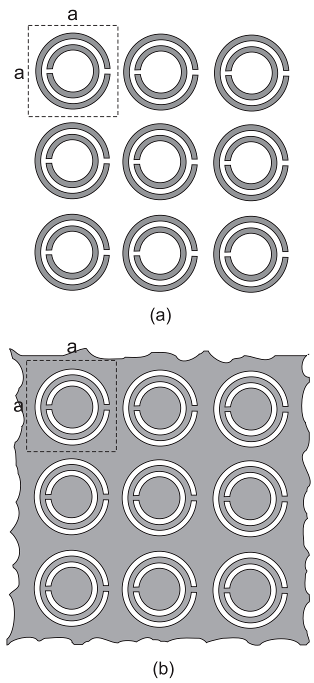

Figure 2. A SRR-FSS (a) and its complementary screen, or CSRR-FSS (b).

$$J_{{\rm s},x} = -{\rm i}\omega\frac{\alpha_{xx}^{ee}}{a^2}E_x - \frac{\alpha_{yz}^{em}}{a^2}\frac{\partial E_y}{\partial y} - {\rm i}\frac{\alpha_{zz}^{mm}}{\omega a^2}\left\{\frac{\partial^2 E_y}{\partial x \partial y} - \frac{\partial^2 E_x}{\partial y^2}\right\} \tag{9}$$

$$J_{{\rm s},y} = -{\rm i}\omega\frac{\alpha_{yy}^{ee}}{a^2}E_y + \frac{\alpha_{yz}^{em}}{a^2}\frac{\partial E_x}{\partial y} + {\rm i}\frac{\alpha_{zz}^{mm}}{\omega a^2}\left\{\frac{\partial^2 E_y}{\partial x^2} - \frac{\partial^2 E_x}{\partial x \partial y}\right\}, \tag{10}$$

where a is the lattice constant of the FSS. Equations (9) and (10), together with the appropriate boundary conditions at $z \to \pm\infty$, determine the electromagnetic problem of the diffraction for an arbitrary incident wave of fixed frequency ω.

In the previous equations, an arbitrary dependence on the x and y coordinates of the incident field has been supposed. In the particular case of an incident plane wave with $\mathbf{E}^{\rm inc} = \mathbf{E}_0^{\rm inc}\exp({\rm i}\mathbf{k}\cdot\mathbf{r} - {\rm i}\omega t)$, the above equations (9) and (10) reduce to a *surface admittance* condition at $z = 0$. That is,

$$\begin{pmatrix} J_{{\rm s},x} \\ J_{{\rm s},y} \end{pmatrix} = \begin{pmatrix} Y_{xx}, & Y_{xy} \\ Y_{yx}, & Y_{yy} \end{pmatrix} \cdot \begin{pmatrix} E_x \\ E_y \end{pmatrix}, \tag{11}$$

where

$$Y_{xx} = -{\rm i}\omega\left\{\frac{\alpha_{xx}^{ee}}{a^2} + \frac{k_y^2\alpha_{zz}^{mm}}{\omega^2 a^2}\right\} \tag{12}$$

$$Y_{yy} = -{\rm i}\omega\left\{\frac{\alpha_{yy}^{ee}}{a^2} + \frac{k_x^2\alpha_{zz}^{mm}}{\omega^2 a^2}\right\} \tag{13}$$

$$Y_{xy} = -\mathrm{i}\omega \left\{ \frac{\alpha_{yz}^{em} k_y}{\omega a^2} - \frac{k_x k_y \alpha_{zz}^{mm}}{\omega^2 a^2} \right\} \qquad (14)$$

$$Y_{yx} = -\mathrm{i}\omega \left\{ -\frac{\alpha_{yz}^{em} k_y}{\omega a^2} - \frac{k_x k_y \alpha_{zz}^{mm}}{\omega^2 a^2} \right\}. \qquad (15)$$

It is worth noting that, according to (4)–(7), $Y_{xy} = -Y_{yx}^*$ for lossless SRRs, as is imposed by energy conservation.

2.3. The complementary screen and the Babinet principle

As is expected from the non-connected nature of the SRR-FSS, it behaves mainly as a stop band FSS (for the appropriate polarization), with a strong reflection peak at the frequency of resonance of the SRRs. In order to obtain the dual behaviour—i.e. a strong transmission peak at this frequency—the complementary screen (see figure 2) can be used. This complementary screen is made by etching the complementary SRRs (CSRRs) on a metallic plate. For thin and lossless plates, the Babinet principle [13] must hold. This principle states that the total field transmitted by a metallic screen with an arbitrary aperture, added to the total field transmitted by its complementary screen (illuminated by the *complementary* incident wave), gives the incident wave over this last structure. For fields incident on the CSRR-FSS, $\mathbf{E}_c^{\mathrm{inc}}$, $\mathbf{B}_c^{\mathrm{inc}}$, related to the incident fields on the SRR-FSS, $\mathbf{E}^{\mathrm{inc}}$, $\mathbf{B}^{\mathrm{inc}}$, by

$$\mathbf{E}_c^{\mathrm{inc}} = c\mathbf{B}^{\mathrm{inc}} \qquad \text{and} \qquad \mathbf{B}_c^{\mathrm{inc}} = -\frac{1}{c}\mathbf{E}^{\mathrm{inc}}, \qquad (16)$$

the Babinet principle states that the total field of the SRR-FSS, $\mathbf{B}$, and that of the CSRR-FSS, $\mathbf{E}_c$, in the shadowed region, $z > 0$, are related by [13]

$$c\mathbf{B} + \mathbf{E}_c = c\mathbf{B}^{\mathrm{inc}}. \qquad (17)$$

Therefore, the transmission coefficients for the CSRR-FSS, t_c, and for the SRR-FSS, t, are related by $t + t_c = 1$. So

$$t_c = -r \qquad \text{and} \qquad r_c = -t, \qquad (18)$$

where t_c and r_c are the reflection and transmission coefficients for the CSRR-FSS when it is illuminated by the complementary wave (16).

Therefore, as is expected, the transmission and reflection coefficients for the SRR-FSS and for the CSRR-FSS interchange roles (for the *complementary* incident waves), so the SRR-FSS total reflection peak becomes a total transmission peak in the CSRR-FSS. Of course, these results only hold for infinitely thin and lossless screens. However, they can be used as a first approximation for more realistic structures

3. Behaviour at normal incidence

Normal incidence is the simplest case for analysis. In fact, $k_x = k_y = 0$ in (12)–(15), and therefore the surface admittance (11) becomes diagonal. However, even in that case, some interesting characteristics appear. Although no cross-polarization effects can occur (the admittance (11) is diagonal), since α_{yy}^{ee} is resonant and α_{xx}^{ee} is not, the behaviours of the FSS for the two orthogonal polarizations of the incident wave will be quite different: for waves polarized with the electric field parallel to the y-axis (see figure 1) a strong reflectivity is expected near the resonance, whereas for incident waves having the orthogonal polarization it is not. Therefore, for normal incidence and near the resonance, the FSS will act as a polarizer.

In the following we will quantitatively analyse the behaviour of the FSS in the resonant case. The polarization of the incident wave is chosen with $\mathbf{E}^{\mathrm{inc}} = E_0\hat{\mathbf{y}}\exp(\mathrm{i}k_z z - \mathrm{i}\omega t)$, in order to obtain a resonant behaviour in the FSS. For this polarization, according to (12)–(15) and (4)–(7), the FSS is characterized by a scalar surface admittance Y_s, given by

$$\mathbf{J}_s = Y_s\mathbf{E}, \qquad Y_s = -\mathrm{i}\omega\frac{\alpha_{yy}^{ee}}{a^2}. \qquad (19)$$

According with (5) this admittance can be rewritten as

$$Y_s = Y_D + \left(\frac{4\omega d_{\mathrm{eff}}}{\pi\omega_0 a}\right)^2 Y_{LC}, \qquad (20)$$

where

$$Y_D = -\mathrm{i}\omega\varepsilon_0\frac{16r_{\mathrm{ext}}^3}{3a^2} \qquad (21)$$

is the admittance of a metallic disk of radius equal to those of the SRR [12]. The term in the second summand in (20), Y_{LC}, can be written as

$$Y_{LC} = \frac{-\mathrm{i}\omega C}{1-\omega^2 LC}, \qquad C = \frac{1}{2}\pi r_0 C_{\mathrm{pul}} \qquad (22)$$

and corresponds to the admittance of the series connection of the equivalent SRR inductance, L, and capacitance $C = \pi r_0 C_{\mathrm{pul}}/2$ [10], giving the frequency of resonance $\omega_0 = \sqrt{(LC)^{-1}}$. The choice of (21) for the non-resonant part of the SRR admittance (20) is justified by the similarity in behaviour of the SRR and the aforementioned disk far from the resonance [5]. The second summand in (20) accounts for the resonant behaviour near ω_0.

The transmission and reflection coefficients across the FSS, t and r, can be obtained from the above admittance, Y_s, following the standard procedure. They are given by

$$t = 1 + r = \frac{2}{Y_s\eta_0 + 2}, \qquad (23)$$

where $\eta_0 = \sqrt{\mu_0/\epsilon_0}$ is the free space impedance. Equation (23) predicts a total reflection peak at the SRR frequency of resonance ω_0, as well as a total transmission point when the total admittance Y_s vanishes. According to (20) and (22) this total transmission is located at some frequency above the SRR resonance. As was already mentioned, the reported analytical results can be extended to the complementary CSRR-FSSs by using (16)–(18). In that case the expressions for the transmission and reflection coefficients are interchanged for the orthogonal polarization of the incident wave.

In order to verify our analysis quantitatively, the theoretical results obtained for a specific CSRR-FSS were compared with those obtained from the commercial software *CST Microwave Studio*. This comparison is shown in figure 3 for the resonant polarization, i.e. when $\mathbf{E}^{\mathrm{inc}} = E_0\hat{\mathbf{x}}\exp(\mathrm{i}k_z z - \mathrm{i}\omega t)$ (as expected, a near zero transmission coefficient was obtained for the orthogonal polarization at all frequencies). In

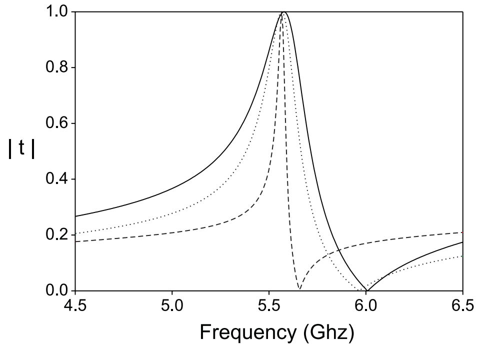

Figure 3. The transmission coefficient for a CSRR-FSS of lattice parameter $a = 8$ mm. The CSRR dimensions are $r_{\rm ext} = 3.5$ mm and $c = d = 0.4$ mm. Solid curve: simulation results obtained using *CST Microwave Studio*. Dashed curve: theoretical results computed from the proposed analytical model with $d_{\rm eff} = c + d$. Dotted curve: results computed using the same model with $d_{\rm eff} = 2(c + d)$.

theoretical computations we have used the design formulae provided in [10] for L and $C_{\rm pul}$, and we have chosen $d_{\rm eff} = c + d$ (dashed curve). A good qualitative agreement can be seen between theoretical and numerical results, as well as an accurate quantitative prediction of the frequency of the transmission peak. The good qualitative agreement includes the zero-transmission point above the transmission peak, although the bandwidth is not accurately predicted. It is worth mentioning that this last disagreement can be overcome by simply adjusting $d_{\rm eff}$, as is shown in the same figure. In fact, the results obtained by taking $d_{\rm eff} = 2(c + d)$ (dotted curve) closely resemble the numerical results. Similar results were obtained for different CSRR dimensions and periodicities. Thus, it can be concluded that the proposed theory qualitatively reproduced the behaviour of the analysed FSSs for normal incidence. It also gives quantitatively accurate predictions for the frequency of resonance, although it underestimates the bandwidth. This fact is probably related to the limitations of the SRR model reported in [5]. Anyway, the overall accuracy of the theory is remarkable, taking into account its analytical nature and the variety of electromagnetic phenomena involved in the structures considered. Thus, we feel that the proposed theory retains most of the physics of the phenomena analysed. However, more theoretical work is still needed for the appropriate quantitative characterization of the bandwidths. Additional support (experimental) for the qualitative predictions of the proposed theory has been reported in [8].

4. Behaviour at oblique incidence

In the oblique incidence case a large variety of cross-polarization effects can be deduced from (11)–(15). In this section we will consider the most important qualitative features for the two orthogonal planes of incidence and the two orthogonal polarizations of the incident waves. Let us first consider the plane of incidence to coincide with the z–x plane of figures 1 and 2. In that case, $k_y = 0$ and the surface admittance (11) is diagonal. Therefore, there are no cross-polarization effects and the reflected and transmitted waves will have the same polarization as the incident one. If the incident wave is polarized in the plane of incidence ($E_y = 0$, $B_x = B_z = 0$), the only relevant polarizability in (1)–(3) is α^{ee}_{xx}. According to (5) this polarizability is non-resonant; therefore it can be neglected in a first approximation and almost no effect is expected for this polarization (the SRR-FSS will be almost transparent). If the incident wave is polarized orthogonal to the plane of incidence ($E_x = E_z = 0$, $B_y = 0$), the relevant polarizabilities are α^{mm}_{zz}, α^{em}_{yz}, and α^{ee}_{yy}. All of these polarizabilities are resonant, and a strong reflection peak will be present at the frequency of resonance of the SRRs. The above results can be directly extended to the complementary screen of figure 2(b) (the CSRR-FSS) by using the Babinet principle (16)–(18). If the incident wave is polarized in the plane of incidence a strong transmission peak is expected at the frequency of resonance of the CSRRs, and an almost opaque surface will be seen for the orthogonal polarization.

Let us now consider incidence in the y–z plane on the SRR-FSS of figure 2(a). In that case $k_y \neq 0$ (and $k_x = 0$). Therefore the non-diagonal terms of the admittance (11) are non-zero, and cross-polarization effects could be present. If the incident wave is polarized in the plane of incidence ($E_x = 0$, $B_y = B_z = 0$) the relevant polarizabilities are α^{ee}_{yy} and α^{em}_{yz}. Both polarizabilities take very high values near the SRR resonance. On substitution in (11) it becomes apparent that both Y_{xy} and Y_{yy} are non-zero. Therefore both components of the surface current $J_{{\rm s},x}$ and $J_{{\rm s},y}$ are excited. Thus, a set of two transmitted and two reflected waves, with orthogonal polarizations, are generated, the FSS showing a strong reflection peak at the frequency of resonance of the SRRs. For the lossless SRRs considered, α^{ee}_{yy} (7) should be real and α^{em}_{yz} (6) imaginary. Therefore $J_{{\rm s},x}$ and $J_{{\rm s},y}$ will be in quadrature, that is, the transmitted and reflected waves will be elliptically polarized. The results for the orthogonal polarization of the incident wave ($E_y = E_z = 0$, $B_x = 0$) are qualitatively very similar. The relevant polarizabilities are now α^{mm}_{zz}, α^{em}_{yz}, and α^{ee}_{xx}. Even neglecting the last of these (it is non-resonant), it is realized that Y_{xx} and Y_{yx} are both non-zero, taking very high values near the SRR resonance. Therefore the same qualitative results as for the polarization in the plane of incidence are expected for the orthogonal polarization. The extension of these results to the complementary screen (the CSRR-FSS of figure 2(b)) is straightforward, and for both polarizations elliptically polarized transmitted and reflected waves are expected, with a strong transmission peak near the CSRR resonance.

5. Conclusions

The behaviour of frequency selective surfaces (FSSs) based on conventional and complementary split ring resonators (SRRs and CSRRs) has been analysed under the approximations of perfectly conducting and infinitely thin metallic screens. In addition to the frequency selectivity, the ability of these devices to act as polarizers and polarization converters has been shown. An analytical model has been proposed for these structures, which is based on the effective admittance concept, as well as on previous results on the SRR polarizabilities. The normal incidence case has been analysed specifically, and the theoretical results compared with numerical results provided by a commercial electromagnetic solver. A good qualitative agreement has been obtained, as well as a very good quantitative prediction of the FSSs resonances (i.e. for the transmission peak of the CSRR-FSS and for the reflection peak of the SRR-FSS). The results for the bandwidth are poorer, although they can be improved by simply adjusting a single parameter of the model. Four orthogonal oblique incidence cases have been discussed, and the most relevant qualitative predictions of the theory, including cross-polarization effects and mode conversion, have been highlighted.

Acknowledgments

This work was supported by the Spanish Ministry of Science and Technology and FEDER funds by project contracts TIC2002-04528-C02-01, TEC2004-04249-C02-01, and TEC2004-04249-C02-02.

References

[1] Wu T K 1995 *Frequency Selective Surfaces and Grid Arrays* (New York: Wiley)
[2] Munk B A 2000 *Frequency Selective Surfaces: Theory and Design* (New York: Wiley)
[3] Pendry J B, Holden A J, Robbins D J and Stewart W J 1999 *IEEE Trans. Microw. Theory Tech.* **47** 2075
[4] Smith D R, Padilla W J, Vier D C, Nemat-Nasser S C and Schultz S 2000 *Phys. Rev. Lett.* **84** 4184
[5] Marqués R, Medina F and Rafii-El-Idrissi R 2002 *Phys. Rev.* B **65** 144440
[6] G-Balmaz Ph and Martin O J F 2002 *J. Appl. Phys.* **92** 2929
[7] Yen T J, Padilla W J, Fang N, Vier D C, Smith D R, Pendry J B, Basov D N and Zhang X 2004 *Science* **303** 1494
[8] Falcone F, Lopetegi T, Laso M A G, Baena J D, Bonache J, Beruete M, Marqués R, Martín F and Sorolla M 2004 *Phys. Rev. Lett.* **93** 197401
[9] Marqués R, Medina F and Rafii-El-Idrissi R 2003 *J. Appl. Phys.* **94** 2770
[10] Marqués R, Mesa F, Martel J and Medina F 2003 *IEEE Trans. Antennas Propag.* **51** 2572
[11] Landau L D and Lifshitz E M 1980 *Statistical Physics* 3rd edn (Oxford: Pergamon)
[12] Collin D R 1991 *Field Theory of Guided Waves* 2nd edn (Piscataway, NJ: IEEE Press)
[13] Jackson J D 1999 *Classical Electrodynamics* 3rd edn (New York: Wiley)